Proceedings of the 17th World Congress
The International Federation of Automatic Control
Seoul, Korea, July 6-11, 2008

Electromechanical Valve Actuator with Hybrid MMF for Camless Engine ⋆

Jieng-Jang Liu† Yee-Pien Yang‡ Jia-Hong Xu⋆⋆

Department of Mechanical Engineering, National Taiwan University, Taiwan.
E-mail: †jjliu@ntu.edu.tw, ‡ ypyang@ntu.edu.tw
⋆⋆*Fan Motor Business Group, Delta Electronic, Inc.*
E-mail: Jhong.Xu@delta.com.tw

Abstract: As one of variable valve timing (VVT) approaches, the electromechanical valve actuator (EMVA) uses solenoid to actuate valve movement independently for the application of internal combustion engine. This paper proposed an EMVA structure by incorporating the hybrid magneto-motive force (MMF) implementation in which the magnetic flux is combined by the coil excitation and permanent magnets. Making use of the dedicated flux arrangement, the proposed device can be used to fulfill the VVT features with reduced power source requirement and less electric device components. A dual flux channels EMVA is detailed and the design procedures are presented. Comparing with the conventional EMV, the proposed prototype shows a lot of advantages such as compactness, high temperature tolerance, fast response, relieve of starting current, and variable current actuating timing.

Keywords: Camless engine; variable valve timing; electromechanical valve actuator; hybrid MMF.

1. INTRODUCTION

Variable valve timing (VVT) has already received much attention from automotive industies and engineers in the past decade. The exploitation and improvement of VVT is one of the effective and essential means for the internal combustion engine with the aim of reducing fuel consumption and exhaust emission. The VVT technologies can be classified into two categories, depending on whether the camshaft is used or not. The VVT without camshaft is also called camless valvetrain. In such a system, the camshaft mechanism is replaced by an electric or hydric system and the freely controls of the duration of valve stroke with possibly infinite variable valve timing can be archieved.

In the conventional EMV system, it is shown by Clark et al. [2005] that the EMV proposed by Wang and Stefanopoulou [2000] and Park et al. [2003] required a high power source to initiate valve movement as the armature stayed at the middle position before the engine starting. A special design for this considerable driving force must be taken in account for ensuring the successful engine starting. Ahn et al. [2005] developed a novel EMV system actuated by the hybrid MMF with permanent magnet (PM) and electromagnet (EM) where a gain-scheduled PID control strategy was proposed to address the soft landing and fast transition issues. Kim and Lieu [2005] proclaimed inherent shortcomings of the conventional EMV system and proposed a new PM based EMV system. Owning to the problem of demagnetization, however, the holding force decreases and became less than the spring force, thereby causing system fault. Jinho and Junghwan [2007] added their new instrument with an embedded magnetic armature. The problem, however, regarding the demagnetization of PM is still not addressed.

Rens et al. [2006] established a novel prototype which had a very special design with a secondary air-gap used for avoiding the flux produced by coils passing through PM. Their design would prevent PM from demagnetization, which had been the main reason causing the system faults, and the proposed EMV system could operate in a high temperature environment. Recently, Lecrivain and Gabsi [2007] proposed many solutions for relieving high starting current as the engine is starting. One of which is the use of parallel polarized PMs and EMs for actuating the valve movement. A secondary air-gap was introduced to avoid demagnetization. In summary, compared with the EMV design without PMs, the hybrid MMF is a promising solution to reduce the consumption of power compared.

The EMVA's can be designed as a hybrid MMF for improving the function of variable valve mechanism, however, the problem of how to get the best performance is still an open issue. In this paper, a suggested type of EMVA is introduced, where the way for PMs to provide electromagnetic force holding the armature is exploited and a secondary air gap is adopted to prevent the PMs from demagnetization. Without current exciting, the valve always keeps in either opened or closed position.

2. NOVEL CONFIGURATION OF EMVA

The proposed prototype can also be classified as a kind of permanent magnet polarized actuators [Rens et al.,

⋆ This work was supported by National Science Council of Taiwan, R.O.C., under Contract NSC 95-2221-E-002-132-MY2.

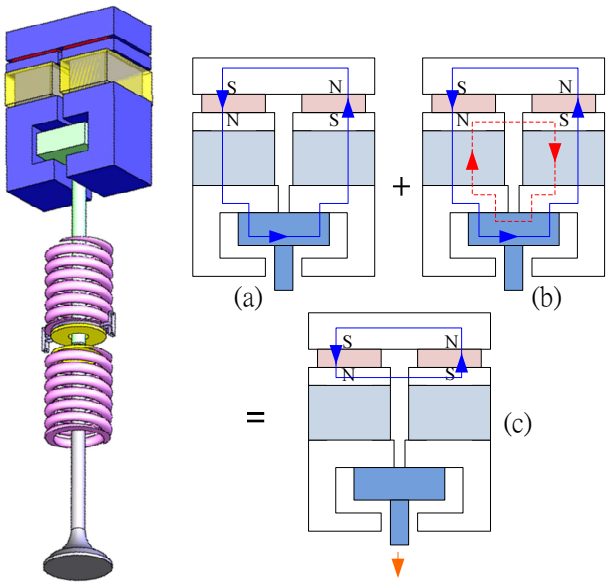

Figure 1. A proposed EMVA with dual flux channels. Loop 1 (solid line) provides force to hold the armature and loop 2 (dotted line) is to release the armature.

2006]. It is designed to have a specific holding force at zero air-gap, as shown in Fig. 1, where the operations incorporting the concept with hybrid MMF (permanent magnet (PM) and electromagnet (EM)) are detailed. As shown in Fig. 1(a), the magnetic flux (loop 1) produced by PMs creates magnetic force to hold the armature to keep the valve closed. Then, when the coils connecting in series are excited by a desired current, the specific magnetic flux (loop 2 in Fig. 1(b)) is induced to weaken the flux produced by PMs so that the armature starts to move towards the other end of stroke. It is worth noting that the flux induced by the coils is directed to pass through a properly designed secondary air gap. Consequently, when the flux passing through the armature decrease to a minimal value, the flux of PM is returned through the air gap so that a reasonable permeance coefficient (PC) value can be guaranteed and the PM will not be demagnetized as shown in Fig. 1(c).

In the conventional designs, the EMV system always needs current exciting to hold the valve in open or closed position, as shown in Fig. 2(a) where the duration of holding time could be up to 80% or more for a single engine cycle. Now, the proposed EMVA is able to drive the valve in a desired trajectory with considerably less electric energy, as illustrated in Fig. 2(b). It is expected that the current exciting is needed only for actuating the movement in an optimal design. No current exciting is required if the valve seated properly. By taking into account the system reliability, however, a small current exciting could be useful for improving the safety operation.

3. DESIGN OF THE EMVA SYSTEM

The proposed configuration of the EMVA, as shown in Fig. 3, consists of the electromechanical device, valve springs, the armature, and position sensor. As an application for internal combustion engine, the specific requirements such as moving speed, accepted noise, and minimized volume space are primary concerned.

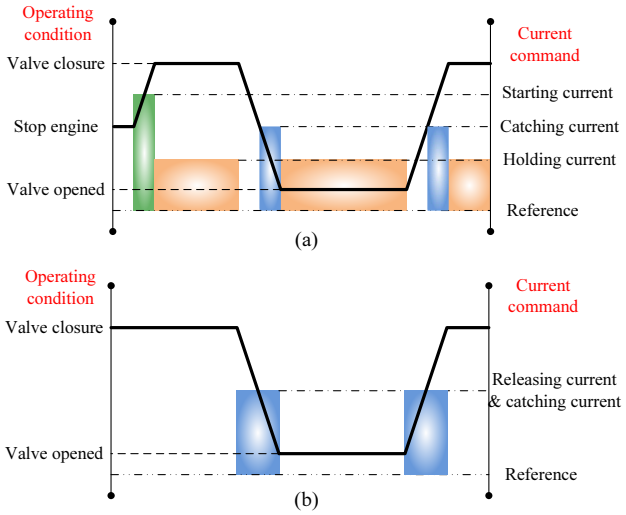

Figure 2. The distribution of drive current: (a) conventional EMV [Jinho and Junghwan, 2007]; (b) the proposed EMV system.

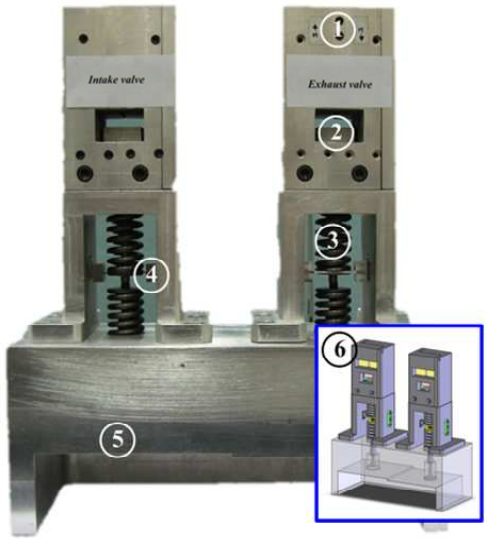

Figure 3. The proposed prototype: (1) electromechanical device; (2) armature; (3) valve springs; (4) position sensor; (5) intake and exhaust valves; (6) CAD diagram.

3.1 Transition time

The transition time, τ_t, is defined as the duration the valve move between two ends. With respect to the engine speed, it can be formulated as

$$\tau_t = \frac{\theta_{\text{open}}}{2} \times \frac{1}{\omega \times (360/60)} \tag{1}$$

For maximum engine speed (ω), the time τ_t can be obtained by the desired valve-open angle θ_{open}, which equivalent to the time that the valve travels the full stroke movement.

3.2 Soft landing

Soft landing is another key point of design. In EMVA system, the mechanical impact between components during the phases of valve landing produces significant acoustic

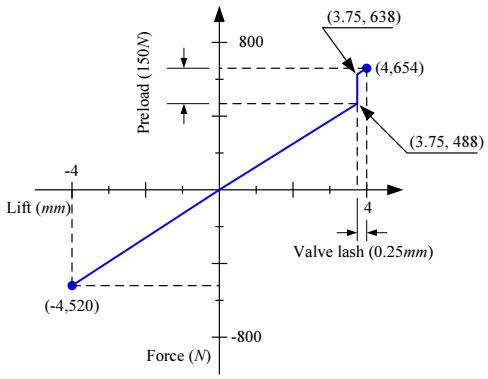

Figure 4. The force with respect to displacement for the preload and valve lash at 130kN/m [Hartwig et al., 2005, Rens et al., 2006].

noise and wear. To avoid the noise and wear, the landing velocity has to be limited in a small value.

3.3 Space limit

It is known that the space available in engine room is limited for all vehicles. In order to replace the traditional camshaft valvetrain with the proposed EMVA system, the optimization for the size of EMVA unit is needed. Taking Mitsubishi Lancer as an example, the valve pitch on the cylinder head is limited 34mm and the altitudinal space available for EMVA assembly is bounded in 0.15m.

3.4 Restricts of the spring stiffness

For high speed engine application, the valve spring with small m/k ratio is required. Theoretically, the ratio is related to the transition time τ_t as

$$\frac{T}{2} = \tau_t = \pi\sqrt{\frac{m}{k}} \tag{2}$$

where T is the period of a cycle, m is the combined mass of armature and valve, and k refers to the spring constant. According to (2), if τ_t is limited in 3.33ms and m is 0.14kg, it is needed that the spring constant of k should be at least 130N/mm for the condition that the engine runs at a speed of 6,000rpm.

For valve spring, the force is proportional to the displacement except in the region of valve lash as shown in Fig. 4. According to the relationship between the force and displacement, the spring constant k can be determined in order that the valves have a desired transition time. Taking the property of thermal expansion on valve stem into account, the design shows that the spring preload is 150N and valve lash has 0.25mm. The detailed specifications are summarized in Table 1.

3.5 Holding force

The holding force, which is exerted by PMs, attracts the armature to the either end of the stroke. In order to maximize the holding force, the flux density between the armature and the steel core is designed to be saturated, which mainly depends on the contact cross-sectional area. Knowing the saturating flux density of the steel, the

Table 1. Specifications of EMVA System

	top position	bottom position
Demandable force	660N	-520N
Revisable force	760N	-620N
Spring constant	65kN/mm	
Transition time	3.33ms	
Moving mass	140g	
Spring preload	150N	
Safety factor	100N	
Valve lash	0.25mm	

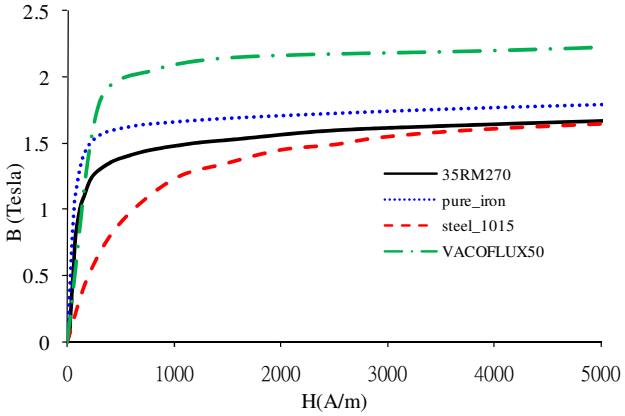

Figure 5. B-H curve for four types of ferromagnetic material [GMBH, 2001].

holding force F between the armature and steel core can be approximated by Cathey [2002].

$$\sum_{i=0}^{n} A_i B_i^2 \cong 2\mu_0 F, \tag{3}$$

where A_i is the contact area and B_i is the flux density passing through A_i. In case that the contact area is constant, the holding force is proportional to the square of the flux density.

Fig. 5 shows the magnetic property of four types of ferromagnetic material. It is seen that the saturating properties are distinct. Among four materials, the silicon steel (35RM270) is laminated and has low eddy current loss while the cost of VACOFLUX50 is high although it has the highest saturated flux density. The mechanical intensity of pure iron is less than the low carbon steel (steel 1015) in spite of that the pure iron has higher magnetic saturating behaviour. Based on these factors, the silicon steel is chosen for steel cores while the low carbon steel is selected for the usage of armature.

4. DYNAMIC MODEL

The electromagnetic analyses, governed by a couple of electrical and mechanical equations are summarized in this section where the electrical equations follow the quasi-static field theory and the mechanical equations are derived from Newton's laws.

4.1 Electrical Subsystem

The electric equation can be expressed as

$$V_s = i(R + R_{\text{coil}}) + \frac{d\lambda}{dt}$$
$$\lambda = N\phi \tag{4}$$
$$\frac{d\lambda}{dt} = L\frac{di}{dt} + vi\frac{dL}{dx}$$

or, equivalently

$$V_s = i(R + R_{\text{coil}}) + L\frac{di}{dt} + vi\frac{dL}{dx} \tag{5}$$

where V_s is the supply voltage, i the input current, R the resistance, R_{coil} the coil resistance, L inductance, and v refers to armature velocity. The variable λ denotes the flux linkage ($\lambda = N\phi$), that is, the total flux linking the circuit.

4.2 Mechanical Subsystem

Taking the free-body diagram of armature, the equation of motion can be expressed in terms of its mass m, viscous friction damping coefficient c, effective spring constant k, top magnetic force $F_{\text{top}}(i,x)$, bottom magnetic force $F_{\text{bottom}}(i,x)$ and gas flow force $F_{\text{flow}}(x)$ acting on the valve. Hence, the equation can be deduced as

$$m\frac{d^2x}{dt^2} + c\frac{dx}{dt} + kx = F_{\text{top}}(i,x) + F_{\text{bottom}}(i,x) + F_{\text{flow}}(x) \tag{6}$$

where the gas flow force $F_{\text{flow}}(x)$ is much smaller than spring force and it is assumed as zero in this study.

4.3 Electromechanical Coupling Subsystem

In order to solve the electrical and mechanical subsystem, the variables $L(x)$, $\partial\lambda(i,x)/\partial x$, $F_{\text{top}}(i,x)$ and $F_{\text{bottom}}(i,x)$ can be expressed in terms of i and x. Letting i and x as independent variables, the coenergy W_c in magnetic field is determined as

$$W_c = \int_{i(0)}^{i(t)} \lambda(i,x)dt \tag{7}$$

and the inductance L can be expressed as

$$L = \frac{\lambda}{i} = \frac{N\phi}{i} \tag{8}$$

Finally, the top or bottom holding force $F(i,x)$ can be deduced as

$$F(i,x) = \frac{\partial W_c}{\partial x} \tag{9}$$

As the magnetic force is designed for the condition with magnetic flux in saturated, it is difficult for mathematical model in (8) to characterize the nonlinearity due to saturation. Accordingly, a look up table deduced from the finite element analysis is adopted to describe the relationship between the magnetic force and displacement in (8).

4.4 Simulation Result

Based on the dynamic model defined from (1) to (9), Fig. 6 shows the three cycles of valve movement with a period of 20ms and a constant current is supplied for releasing the valve at the position between zero and 2mm. The profile characters a flat area at the valve-open and valve-closed position, which is much different from the profile

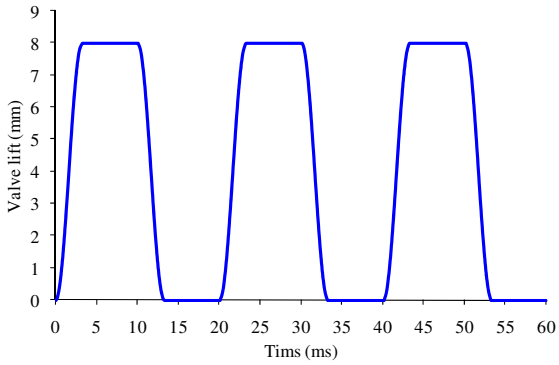

Figure 6. The profile for three cycles of EMVA movement.

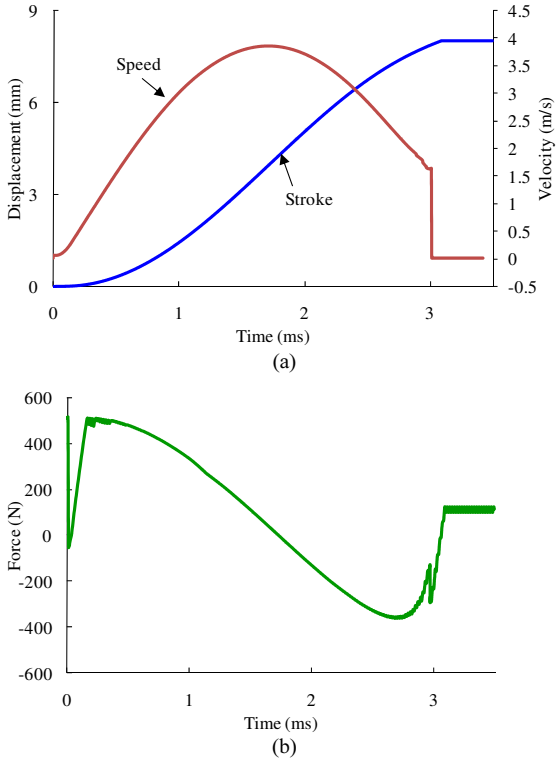

Figure 7. The half cycle of EMVA movement: (a) the stroke and speed as a function of time; (b) the force composed of spring force and magnetic force.

driven by camshaft. Fig. 7 shows the valve movement in a half cycle moves from the valve-open to valve-closed. It is seen that the travelling time of valve is 3.09ms while the impact velocity at valve-closed position is about 1.6m/s due to the attraction force deduced from the PM, as shown in Fig. 7(a). Such a high impact velocity will cause impact noise and serious wearing. Fig. 7(b) shows the total force acting on the armature is composed of spring force and magnetic force, i.e. $F = (F_{\text{top}}(i,x) + F_{\text{bottom}}(i,x) + F_{\text{spring}}(x))$ where the discontinuous point at 3ms is the instance that the valve lash is created due to the separation of valve stem from armature stem.

The experimental setup modelling the valvetrain construction is shown in Fig. 3, where the configuration is composed of an EMVA system, spring trains, a position sensor and a model of cylinder head. The detail physical properties of EMVA are listed in Table 2. To show up

Table 2. Electromechanical Valve Actuator Specifications

Electromechanical coupling subsystem	
Remanence (Br)	1.22T
Coercivity (Hc)	907kA/m
Electrical subsystem	
Supply voltage	42V
Coil	1.1mm 80turns
Mechanical subsystem	
Size (W×L×H)	$34\times54\times78mm^3$
Moving mass	139.6g

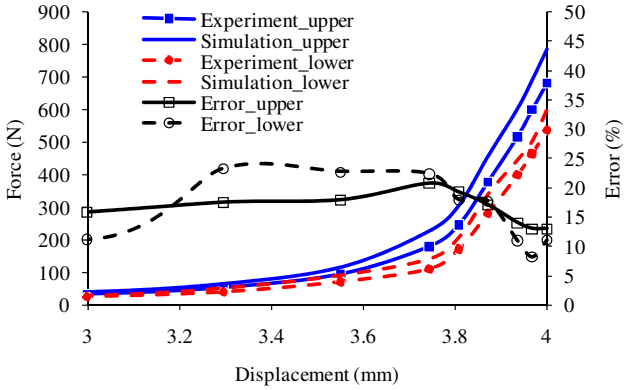

Figure 8. The holding force for the simulation and experiment with zero current exciting. (The total stroke is between -4mm and 4mm. Upper means 0∼4mm while lower indicates 0∼-4mm.)

the detailed profiles of magnetic force, the experimental instrument "Material Test System (MTS)" is used for the measurement of force vs. displacement. The force in relation to armature displacement without current exciting is given in the first stage and the force in relation to various current on the valve-closed position is given as the second. Based on the results, the detailed curves of the force can be built.

Fig. 8 shows the experimental results of the holding force at valve-open and valve-closed positions, respectively. With respect to the position, the force profile indicates that the top force is given 680N, and the bottom is in 534N.

Comparing with the simulated results, the error of the top force is approximately 12% and that of the bottom is approximately 13%; both are less than the predicted results by FEA. Such error is caused by some parasitic air-gaps in the magnetic loop at the location that the armature and steel cores contact each other.

Fig. 9 shows the variation of holding force vs. current inputs for valve-open and valve-closed positions, respectively. In condition that the current increases, the magneto-motive force will decrease due to an opposite magneto-motive force is deduced by current exciting. In other words, before the flux density of the armature to be saturated (or equivalently, the flux density vs. current exciting is linear), the results of simulation and experiment will become more similar. As a result, the error is decreased by increasing current.

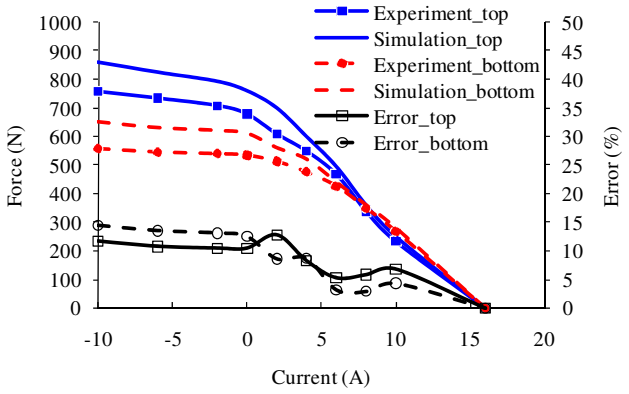

Figure 9. The holding force with respect to current exciting for the simulation and experimental results. (Top is @4mm; bottom is @-4mm.

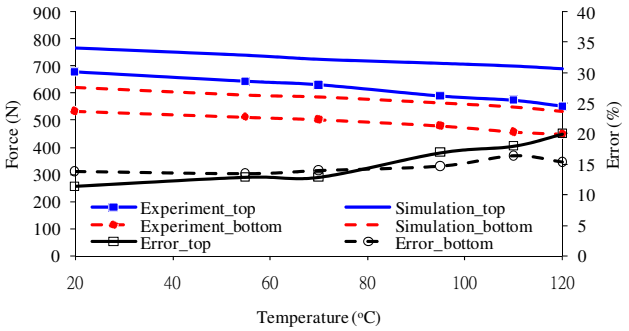

Figure 10. The holding force with respect to the variation of temperature. (Top is @4mm; bottom is @-4mm. Force is an absolute value.)

For high temperature, the B-H curve of magnet decays somewhat from low to high temperature, which is known as an effect of demagnetization. Therefore, the effect of high temperature in holding force must be taken into account for the design of proposed EMVA. Fig. 10 presents the experimental force, compared with the simulated results from FEA for the temperature between 20°C and 120°C. It is found that the holding force decreases as the temperature increases.

The error of the measured holding force is approximately 15% both for top or bottom position. The top force will decrease 1.28N/°C, and the bottom will decrease 0.84N/°C. The discrepancy of experimental results has the same tendency as those in simulation results while the temperature is decreasing.

Without the feedback control, an experimental operation is performed by applying a simplified current exciting command to exam the characteristic for the proposed prototype. Fig. 11(a) shows the desired current profile (i_c), experimental input current (i_a) and their associated deviation ($i_a - i_b$). In the experiment, the slower sampling rate is limited by the ability of experimental hardware so that the maximum deviation of current is approximately 3.7A. For higher sampling rate, the better performance of controlled input current can be archived.

Fig. 11(b) shows that there exists a impact velocity of 0.69m/s as the valve moving a full stroke from the top to bottom position. Due to the open loop control, such

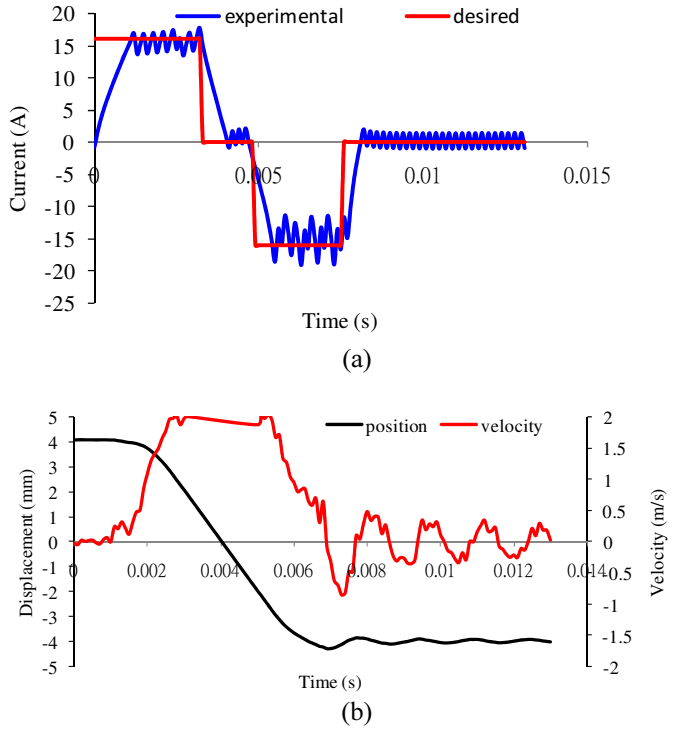

Figure 11. Experimental results of EMVA system: (a) desired input current and real input current; (b) The trajectory for valve displacement and velocity for moving from top to bottom position.

a landing velocity is inevitable. In order to have an acceptable controlled performance, a properly feedback control strategy is required.

5. CONCLUSION

A new EMVA system is proposed with significant improvements then conventional ones. First of all, the need of enormous current for system starting is excused as the valves are always kept in valve-closed position before engine starts. The PM's provide the force holding the armature with no current supplied into the coil. As a result, the issue of high power source requirement for conventional EMVA systems is solved. Secondly, the demagnetizing problem can be addressed by a specific construction prototype for high current exciting operations. The flux is designed as an additional path when the current is excited for releasing and catching the valve.

A novel current input pattern is proposed where the advantages of the PM and EM hybrid system are taken in account. Moreover, a preliminary PM dual channel parallel polarized EMVA system was manufactured and verified.

REFERENCES

H. J. Ahn, Kwak S. Y., J. U. Chang, and D. C. Han. A new EMV system using a PM/EM hybrid actuator. In *Proceedings of the 2005 IEEE International Conference on Mechatronics*, pages 816–821, Taiwan, Taipei, 2005.

J. J. Cathey. *Electric Machines: analysis and design applying matlab*. McGraw-Hill, Boston, 2002.

R. E. Clark, Jewell G. W, S. J. Forrest, J. Rens, and C. Maerky. Design features for enhancing the performance of electromagnetic valve actuation systems. *IEEE Transactions on Magnetics*, 41(3):1163–1168, 2005.

VACUUMSCHMELZE GMBH. *Soft Magnetic Cobalt-Iron-Alloys*. VACUUMSCHMELZE GMBH & CO. KG, Hanau, Germany, 2001.

C. Hartwig, O. Josef, and K. Gebauer. Dedicated intake actuator for electromagnetic valve trains. *SAE*, 2005. 2005-01-0773.

K. Jinho and C. Junghwan. A new electromagnetic linear actuator for quick latching. *IEEE Transactions on Magnetics*, 43(4):1849–1852, 2007.

J. Kim and D. K. Lieu. Designs for a new quick-response latching electromagnetic valve. In *Proceedings of the 2005 IEEE International Conference on Electric Machines and Drives*, pages 1773–1779, San Antonio, TX, United States, 2005.

M. Lecrivain and M. Gabsi. Electomagnetic actuator for controlling a valve of an internal combustion engine and internal combustion engine equipped with such an actuator. *USPTO*, 2007. US 7.156.057B2.

S. H. Park, J. Lee, J. Yoo, D. Kim, and K. Park. Effects of design and operating parameters on the static and dynamic performance of an electromagnetic valve actuator. *Proceedings of the Institution of Mechanical Engineers, Part D: Journal of Automobile Engineering*, 217:193–201, 2003.

J. Rens, R. E. Clark, and G. W. Jewell. Static performance of a polarized permanent-magnet reluctance actuator for internal combustion engine valve actuation. *IEEE Transactions on Magnetics*, 42(8):2063–2070, 2006.

Y. Wang and A. G. Stefanopoulou. Modeling of an electromechanical valve actuator for a camless engine. In *Proceedings of the 5th international Symposium on Advanced Vehicle Control*, 2000.